

Least Squares-Filtered Bayesian Updating for Remaining Useful Life Estimation

Alexandra Coppe¹, Raphael T. Haftka², and Nam-Ho Kim³
University of Florida, Gainesville, FL, 32611

Information on damage size and growth obtained using structural health monitoring can be used to estimate remaining useful life (RUL). Damage growth information may also be used to improve the characterization of the material properties that govern damage propagation for the structure being monitored, turning aircraft into flying fatigue laboratories. These properties are often widely distributed between nominally identical structures because of differences in manufacturing processes and aging effects. The improved accuracy in damage growth characteristics allows more accurate prediction of the RUL of the monitored structural component. It can also help in anticipating damage growth on other similar components. Bayesian inference has been used for progressively reducing the uncertainty in structure-specific damage growth parameters in spite of noise and bias in sensor measurements. However, Bayesian updating is computationally intensive and may not be feasible to use with an extremely large number of measurements. Least squares fitting of the damage growth parameters, on the other hand is efficient, but does not provide good statistical information on the uncertainty in their estimates and in RUL estimates. In this paper we propose combining the two approaches by using the least-squares approach to filter data for the Bayesian updating.. The approach is applied to crack growth in fuselage panels due to cycles of pressurization and depressurization. It is shown that the proposed method rapidly converges to the accurate damage parameters when the initial damage size is 20mm. Fairly accurate damage parameters can be obtained also with measurement errors of 5mm. Using the identified damage parameters, it is shown that the 95% conservative RUL converges to the true RUL from the conservative side.

Nomenclature

Δa_N	=	Damage growth at N th inspection
Δa_N^{meas}	=	Measured damage growth at N th inspection
ΔK	=	Range of stress intensity factor
$\Delta \sigma$	=	Range of applied stress
Δp	=	Pressure differential
a	=	Half damage size
a_C	=	Critical crack size
a_i	=	Initial crack size
a_N	=	Crack size at N th inspection
a_N^{meas}	=	Measure crack size at N th inspection
a_N^{true}	=	Modeled crack size at N th inspection
b	=	Bias in measurements
C	=	Paris law parameter
K_{IC}	=	Fracture toughness
m	=	Paris law exponent

¹ Graduate research assistant, Mechanical and Aerospace Engineering department, University of Florida, Gainesville, FL, 32611, AIAA Student Member.

² Distinguished Professor, Mechanical and Aerospace Engineering department, University of Florida, Gainesville, FL, 32611, AIAA Fellow.

³ Associate Professor, Mechanical and Aerospace Engineering department, University of Florida, Gainesville, FL, 32611, AIAA Member.

N	=	Number of cycles
N_f	=	Remaining useful number of cycles
r	=	Fuselage radius
t	=	Panel thickness
v	=	Noise in measurements
V	=	Amplitude of noise in measurements

I. Introduction

STRUCTURAL health monitoring (SHM) will have significant impact on increasing safety as well as reducing operating and maintenance costs by providing an accurate quantification of degradation and damage at an early stage to reduce or eliminate malfunctions. Furthermore, SHM will allow predictions of the structure's health status and remaining useful life (RUL) without intrusive and time consuming inspections. Continual on-line SHM is based on dynamic processes through the diagnosis of early damage detection, then prognosis of health status and remaining life.

Once the damages reach detectable size, various SHM techniques can be employed to evaluate the current state of structural health by measuring the size of damages¹. In the physics-based prognosis techniques, it is necessary to incorporate the measured data into a damage growth model to predict the future behavior of the damage.

Prognosis techniques can be categorized based on the usage of information: (1) physics-based, (2) data-driven, and (3) hybrid methods. A physics-based method, or model-based method², assumes that a model of system behavior is available and combine this model with measure data to identify system characteristic and predict future behavior. Dynamic stochastic equation, lumped-parameter model³, and functional models⁴ correspond to this category. In the case of SHM, crack growth model^{3, 5, 6} or spall growth models are often used for micro-level damage, and first principle models⁷ are used for macro-level damage.

A data-driven method⁸ uses information from collected data to predict future status of the system but does not use any particular physical model. It includes least-square regression^{9, 10}, Gaussian process regression^{11, 12}, neural network^{7, 11, 12}, and relevance vector machine^{11, 13}. This type of method has advantages when the system is so complex that no simple physical model is available. The hybrid method¹⁴ combines the abovementioned two methods, and includes particle filters¹⁵ and Bayesian techniques^{16, 17}. It is generally accepted that managing uncertainty is the most challenging part for prognosis^{17, 18}. Sources of uncertainty are initial state estimation, current state estimation, failure threshold, measurement, future load, future environment, and models. In order to manage the uncertainty, various methods have been proposed, such as confidence intervals¹⁹, relevance vector machine¹¹, Gaussian process regression^{11, 12}, and particle filters^{15, 20}. Since structural damage grows slowly and the physics governing its behavior is relatively well-known, the physics-based method is used in this paper.

The current technology of diagnosis and prognosis using SHM anticipates difficulties associated with uncertainties in sensor data, damage growth models, and material and geometric properties. The first is related to identifying the current health status, while the others are related to predicting the health status in the future. Uncertainties in sensor data can be classified in two categories: systematic departure due to bias and random variability due to noise. The former is caused by calibration error and device error, while the latter is caused by measurement environment.

Compared to manual inspections, the accuracy of SHM is still poor. The minimum size of detectable damages of SHM is much larger than that of manual inspection methods. In addition, the measured data have the abovementioned noise and bias. Thus, the major challenge in SHM-based prognosis is how to accurately predict the damage growth when the measured data include both noise and bias. However, unlike manual inspection, SHM may provide frequent measurement of damage, allowing us to follow damage growth. This in turn, should allow us to reduce the uncertainty in the material properties that govern damage growth. As illustrated in Figure 1 the uncertainty in these properties is normally large because of variability in manufacturing and ageing of the monitored structure²¹.

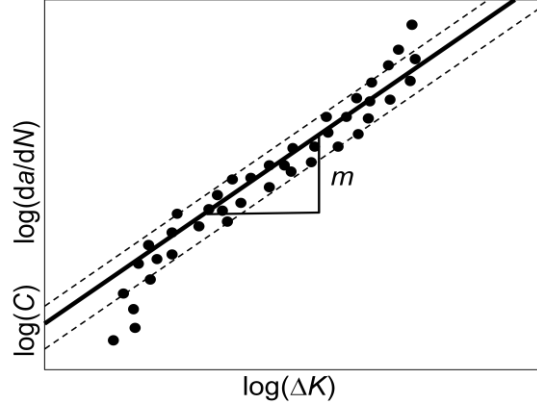


Figure 1. Illustration of Paris law parameter in a log-log plot of crack growth rate

The main objective of this paper is to demonstrate the reduction in uncertainty that may be achieved with SHM data combining Bayesian inference with least square fit identification. A probabilistic approach using Bayesian statistics is first employed to progressively improve the accuracy of predicting damage parameters under noise and bias of sensor measurements. That method encounters difficulties when it comes to large sets of data and biased data. It is then compared to the least square fit identification method, which is good to identify deterministic parameters rather than distributions. The two methods are then combined for a final goal of identifying the damage parameter distribution with enough accuracy to give us a conservative estimate of the remaining useful life of the structure.

The approach is demonstrated for a through-thickness crack in an aircraft fuselage panel which grows through cycles of pressurization and de-pressurization. A simple damage growth model, Paris law, with two damage parameters is utilized. However, more advanced damage growth models can also be used, which usually comes with more parameters. Using this simple model we aim to demonstrate that SHM can be used to identify the damage parameters of a particular panel. This process can be viewed as turning every aircraft into a flying fatigue laboratory. Reducing uncertainty in damage growth parameters can reduce in turn the uncertainty in predicting remaining useful life (RUL); i.e., in prognosis.

The paper is organized as follows. In Section 2, a simple damage growth model based on Paris model is presented. The current paper is based on data for the fatigue crack growth in a fuselage panel of 7075-T651 aluminum alloy. In Section 3 the results are given for least square fit method, on the identification of the damage parameters and the estimate on remaining useful life. In Section 4 the corresponding results are given for Bayesian updating. In section 5, comparable results are presented obtained using a least-square-based Bayesian method. Conclusions are presented in Section 6 along with future plans.

II. Damage growth and measurement uncertainty models

A. Damage growth model

Damage in a structure starts at the microstructure level, such as dislocations and gradually grows to the level of detectable macro-cracks through nucleation and growth. Damage in the micro-structure level grows slowly, is often difficult to detect, and is not dangerous for structural safety. Thus, SHM often focuses on macro-cracks, which grow relatively quickly under fatigue loadings.

In this paper, we consider a fatigue crack growth in a fuselage panel with initial crack size a_i subjected to fatigue loads with constant amplitude due to pressurization. The hoop stress varies between a maximum value of σ to a minimum value of zero in one flight. One cycle of fatigue loading represents one flight. Like many other researchers^{22,23}, we use the damage growth model²⁴ as

$$\frac{da}{dN} = C(\Delta K)^m \quad (1)$$

where a is the half crack size in *meter*, N the number of cycles (flights), da/dN the crack growth rate in *meter/cycle*, and ΔK the range of stress intensity factor in $MPa\sqrt{meter}$. The above model has two damage growth parameters, C and m . The plot of $\log(da/dN)$ versus $\log(\Delta K)$ becomes a straight line with m being the slope and $\log(C)$ being the y-intercept at $\log(\Delta K) = 1$.

The range ΔK of stress intensity factor for a center-cracked panel is calculated as a function of the stress $\Delta\sigma$ and the half crack length a in Eq. (2), and the hoop stress due to the pressure differential Δp is given by Eq. (3)

$$\Delta K = \Delta\sigma\sqrt{\pi a} \quad (2)$$

$$\Delta\sigma = \frac{(\Delta p)r}{t} \quad (3)$$

where r is the fuselage radius, and t is the panel thickness. Equation (2) does not include a geometric correction factor due to the finite size of the panel, and Eq. (3) does not include corrections due to the complexity of the fuselage construction, so that they are both approximate.

The number of cycles N of fatigue loading that grows a crack from the initial half crack size a_i to the current half crack size a_N can be obtained by integrating Eq. (1).

$$N = \int_{a_i}^{a_N} \frac{da}{C \Delta\sigma\sqrt{\pi a}^m} = \frac{a_N^{1-m/2} - a_i^{1-m/2}}{C(1-m/2)(\Delta\sigma\sqrt{\pi})} \quad (4)$$

Alternatively, the half crack size a_N after N cycles of fatigue loading can be obtained by solving Eq. (4) for a_N .

$$a_N = \left(NC \left(1 - \frac{m}{2} \right) \Delta\sigma\sqrt{\pi}^m + a_i^{1-m/2} \right)^{\frac{2}{2-m}} \quad (5)$$

It is assumed that the panel fails when a_N reaches a critical half crack size, a_c . Here we assume that this critical crack size is when the stress intensity factor exceeds the plane-strain fracture toughness K_{IC} . This leads to the following expression for the critical crack size (again neglecting finite panel effects)

$$a_c = \left(\frac{K_{IC}}{\Delta\sigma\sqrt{\pi}} \right)^2 \quad (6)$$

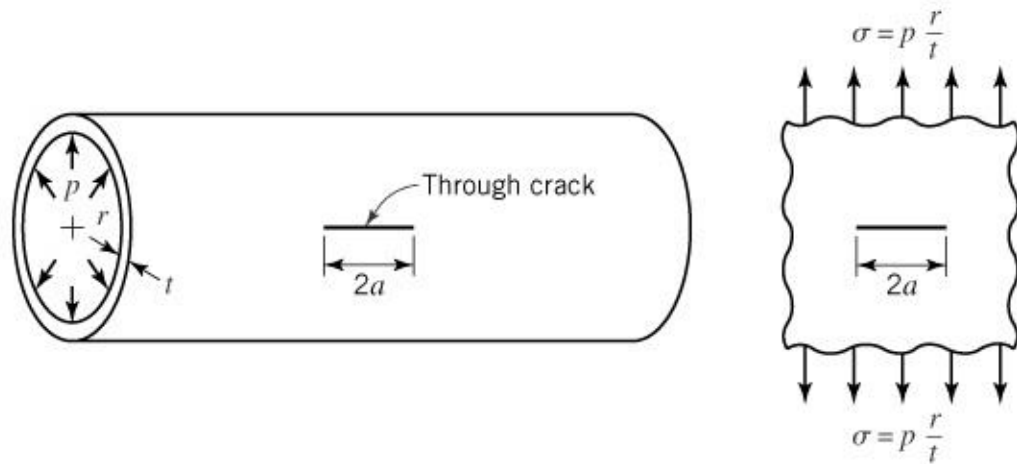


Figure 2. Through the thickness crack illustration

Typical material properties for 7075-T651 aluminum alloy are presented in Table 1. The applied fuselage pressure differential is 0.06 MPa, obtained from Niu²⁵ and the stress is given by Eq. (3). Paris parameters m and C are obtained using a crack growth rate plot published by Newman, et al.²⁶. Note that due to scatter in the data, the exponent m and $\log(C)$ are assumed to be uniformly distributed between the lower- and upper-bounds. Although it is well known that the two Paris parameters are correlated²⁷, this effect is not considered in this paper because we try to identify one parameter assuming the other parameter is known. In the future work, we will address identifying both parameters simultaneously.

Table 1. Geometry, loading and fracture parameters of 7075-T651 Aluminum alloy

Property	Pressure* Δp (MPa)	Fracture toughness K_{IC} (MPa \sqrt{m})	Fuselage radius r (meters)	Paris law exponent m	Damage parameter $\log(C)$
Distribution type	Lognormal (0.06, 0.003)	Deterministic 30	Deterministic 3.25	Uniform (3.3, 4.3)	Uniform ($\log(5E-11)$, $\log(5E-10)$)

*Modeled as constant in simulations.

B. Measurement uncertainty model

In general, cracks in fuselage panels grow according to the repeated pressurizations. Then, the structural health monitoring (SHM) system that is composed of sensors and actuators may detect these cracks. The fundamental function of SHM is to detect these cracks before they become unstable and dangerous. The main objective of this paper is to show that the measured data can be used to identify crack growth parameters, and then, to predict the future behavior of the cracks.

Since no airplanes are equipped with SHM systems yet, we simulate the measured crack sizes from SHM. In general, the measured damage includes the effect of bias and noise of the sensor measurement. The former is deterministic and represents a calibration error, while the latter is random and represents a white noise. The synthetic measurement data are generated by (1) assuming that the true parameters, m_{true} and C_{true} , are known, (2) calculating the true crack growth according to Eq. (5) for a given N , and (3) adding a deterministic bias and random noise. Let a_N be the true half crack size, b the bias, and v the noise. The measured half crack size, a_N^{meas} , is then given as

$$2a_N^{meas} = 2a_N + b + v \quad (7)$$

For subsequent measurements, the bias b remains constant, while the noise v is assumed to vary uniformly with maximum range V . Let the measurement interval be ΔN . Then, the measured damage sizes can be used to define the damage growth between consecutive inspections as follows

$$\Delta a_N^{meas} = a_N^{meas} - a_{N-\Delta N}^{meas} = \Delta a_N - \Delta v_N \quad (8)$$

If the measured crack sizes are uniformly distributed due to the noise, then the measured crack growths are triangularly distributed with mean at the true crack growth. Thus, the respective distributions of the measured crack size and crack growth can be found below:

$$\begin{cases} a_N^{meas} \sim U \ a_N + b/2 - V/2; a_N; a_N + b/2 + V/2 \\ \Delta a_N^{meas} \sim T \ \Delta a_N - V; \Delta a_N; \Delta a_N + V \end{cases} \quad (9)$$

The objective is to identify the true crack growth parameters using the measured crack size and its growth in Eq. (9). Once these parameters are identified, they can be used to predict the remaining useful life. Since we simulate what we called measured data because of the lack of actual data, we repeat this process multiple times to simulate the actual data statistically. Accordingly, the results will also be presented in terms of probabilistic distribution.

III. Characterization of damage properties using Bayesian updating

Depending on manufacturing and assembly processes, the actual damage parameters for individual aircraft can be different. For a specific panel, we assume that there exists a true value of deterministic damage parameters. In the following numerical simulation, the true damage will grow according to the true value of damage parameters. On the other hand, the measured damage size will have bias and random noise in the measurements. As a first approach to the problem we consider the distributions of m and C separately, which means that when we consider one variable as being uncertain, we assume that the other one is known.

From a preliminary damage growth analysis, it was found that the effect of noise in pressure p has negligible effect on damage growth because the effect of randomness is averaged out. This is true for fuselage pressurization because the variation is small. Thus, in the following analysis, the applied pressure is assumed to be deterministic, 0.06 MPa, the mean value of the distribution obtained from Niu²⁵.

In general, the minimum size of detectable damage using SHM is much larger than that of the manual inspection. Although different SHM techniques may have different minimum detectable size, we choose an initial half crack size $a_0 = 10$ mm, which is large enough to be detected by most SHM methods. In addition, this size of damage will provide significant crack growth data between the two consecutive inspections.

The damage growth parameter m is a critical factor to determine the growth of damage. This parameter is normally measured using fatigue tests under controlled laboratory tests. However, uncertainty in this parameter is normally large not only at a material level because of variability in manufacturing and aging of the specific panel, but also on a specimen level because of variability related to testing process. It is possible to curve fit the data and obtain estimates of this parameter for the individual panel. However, curve fits do not take into account prior information on the distribution of these parameters or statistical information on the measurement uncertainty. In this paper, we use Bayesian inference to identify these parameters, which can take into account both effects.

As can be seen in Figure 1, the exponent m is the slope of the curve in the log-log scale. As a first step in developing a prognosis methodology, we assumed that the accurate value of C is known, while that of m is uncertain. Since the range of the exponent m is generally known from literature or material handbooks, we assume that the exponent is uniformly distributed between the lower- and upper-bounds. Then, the goal is to narrow the distribution of the exponent using the Bayesian statistics with measured damage sizes. The data used for the updating of material properties are crack growth calculated from two measurements as defined in Eq.(8) with uncertainty defined in Eq. (9).

Bayesian inference is based on the Bayes' theorem on conditional probability. It is used to obtain the updated (also called posterior) probability of a random variable by using new information. In this paper, since the probability distribution of m given Δa is of interest, we used the following form of Bayes' theorem²⁸:

$$f_{updt} m = \frac{l \Delta a | m f_{ini} m}{\int_{-\infty}^{+\infty} l \Delta a | m f_{ini} m dm} \quad (10)$$

where, f_{ini} the assumed (or prior) probability density function (PDF) of m , f_{updt} the updated (or posterior) PDF of m and $l(\Delta a|m)$ is called the likelihood function, which is the probability of obtaining the measured damage growth, Δa , for a given value of m .

The likelihood function is designed to integrate the information obtained from SHM measurement to the knowledge we have about the distribution of m . The details of the derivation and calculation of the likelihood function can be found in Appendix A. Instead of assuming an analytical form of the likelihood function, we propagate uncertainty in measured crack sizes and estimated using the Monte Carlo simulation (MCS). Although this process computationally expensive, it will provide accurate information for the posterior distribution (refer to Appendix A).

Once the distribution of m has been identified at cycle N , it can be used to predict the remaining useful life (RUL). The distribution of RUL is calculated at every SHM measurement cycle N using MCS as well but with a larger sample than the one used to calculate the likelihood function, 50,000 true crack sizes are estimated using the following distribution in Eq. (11) and the RUL is estimated using Eq. (12) derived from Paris' law. This allows us to estimate the distribution and from there obtain the 5th percentile.

$$a_N^{true} \sim U(a_N^{meas} - V/2; a_N^{meas} + V/2) \quad (11)$$

$$N_f = \frac{a_C^{1-m/2} - a_N^{true \ 1-m/2}}{C \left(1 - \frac{m}{2}\right) \sigma \sqrt{\pi}} \quad (12)$$

Once the PDF of m is obtained, it can be used to predict the RUL of the monitored panel. Since the PDF is updated at every SHM measurement, the predicted RUL will vary at every measurement interval ΔN . In predicting RUL, 50,000 samples of m , a_N^{true} , and σ are generated, and Eq. (12) is used to calculate samples of N_f . In order to have a safe prediction of RUL, 5th percentile of N_f samples is used as a conservative estimate of RUL. Since we used synthetic data by adding random noise, the result may vary with different sets of data. Thus, the above process is repeated with 100 sets of measurement data and mean \pm one standard deviation intervals are plotted. In order to show the value of our method we compare RUL calculated using the actual value of m , m_{true} , and the distribution (mean \pm one standard deviation) of the 5th percentile of the distribution of RUL obtained using the updated distribution of m at each inspection, for the case of negative bias, -2mm and a noise of amplitude 1mm, this is shown in Figure 3. It can be observed that Bayesian updating allows us to improve the estimation of RUL compared to the RUL obtained using the handbook distribution, that estimation converges to the true RUL from the conservative side but it is sensitive to error in the data.

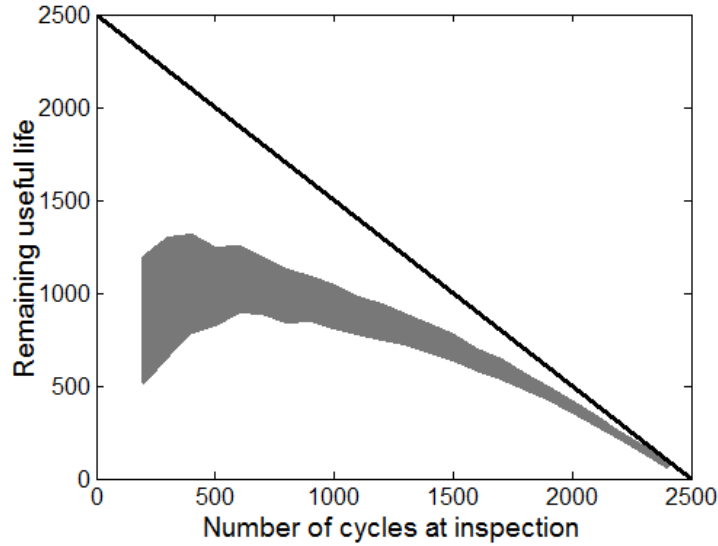


Figure 3. Distribution (mean \pm one standard deviation) of the 5th percentile of RUL for $b = -2\text{mm}$ and $V = 1\text{mm}$, using Bayesian updating

One of the major advantages of SHM is that measurements can be performed frequently. Thus, the update in Eq. (10) can be performed as frequently as needed. However, since the damage grows slowly and the bias and noise of measurements are in general large, too frequent measurements may not help to narrow down the distribution of damage parameters because Bayesian inference does not give good results with large samples of data.

IV. Characterization of damage properties using least square fit

In the previous section, Bayesian inference is used to identify a single damage growth parameter, either m or C , and assumed the other parameter is already known. In practice, when both parameters are unknown, Bayesian inference needs to update the joint PDF of both parameters. In general, this can be achieved by dividing the ranges of uncertain parameters into a grid and calculate the joint PDF value at each grid point. If the range is divided by 100×100 grid, the updating process includes 10,000 times calculation of likelihood, requires uncertainty propagation for given parameter values. Thus, the updating process easily becomes computationally impractical. In addition, in the previous section, the bias and initial true crack size are considered uncertain because their value is unknown. In theory, they can also be treated similarly to damage growth parameters and be identified through Bayesian inference. Then, the four-dimensional joint PDF needs to be updated, which is computationally impractical. Before we present a new method of addressing this computational issue, we will present a conventional method of identifying unknown parameters in this section, along with its advantages and disadvantages.

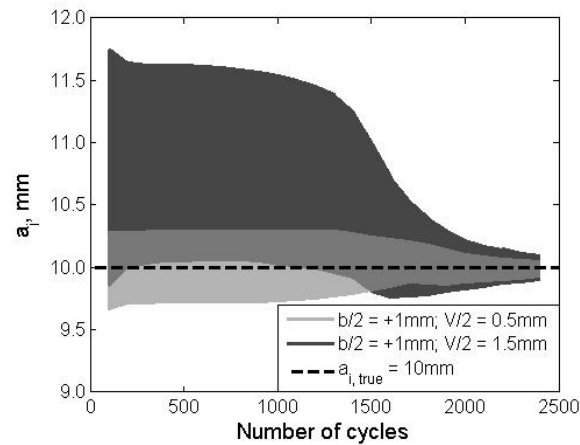
Least square fit is the easiest and most commonly used way of identifying model parameters by minimizing the difference between measured data and predicted data from the physics model. In our application, the Paris model is used with the following unknown parameters: initial crack size, a_0 , damage growth parameter, m , and bias, b . The parameter C is still assumed to be known in order to compare with the results in the previous section. The least square fit problem can be formulated as

$$\min_{a_0, m, b} \sum_i a_i^{meas} - b - a_i^2 \quad \text{with } a_i = \left[NC \left(1 - \frac{m}{2} \right) \sigma \sqrt{\pi}^m + a_0^{1-\frac{m}{2}} \right]^{\frac{2}{2-m}} \quad (13)$$

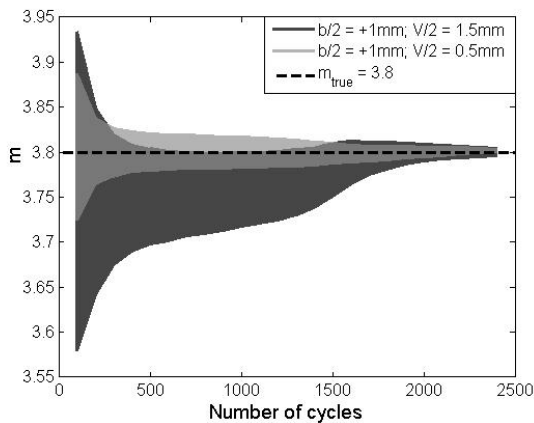
In order to have the same configuration with Bayesian inference, the initial range of parameter m is used as lower- and upper-bounds. The bounds of bias are chosen between -2 and 2mm as we assume that this is reasonable estimate of the bias. Since the initial crack size is within the combined ranges of bias and noise from the measured initial crack size, its lower- and upper-bounds are selected accordingly. The least square fit is performed using lsqnonlin function in MATLAB. At measurement cycle N , all previous measurement data are used in the least square fit. Thus, more and more data are used in least square fit as the number of cycles increases. Although

Bayesian inference is performed at every $\Delta N = 100$ interval, the least-square-fit is performed at every cycle because the accuracy of fitting is better with more data.

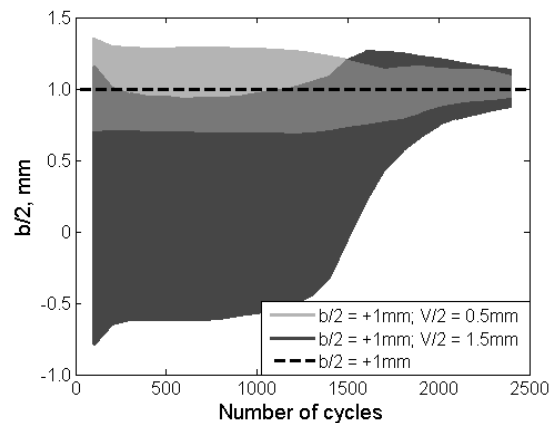
Similar to Bayesian inference, the identified parameters depend on synthetic measurement data. Thus, 1,000 sets of measurement data are produced by adding deterministic bias and random noise to the true crack sizes. Thus, at every measurement cycle, there exist 1,000 number of identified parameters. In order to show how these parameters are distributed, Figure 4 shows intervals of mean \pm one standard deviation for two different combinations of noise and bias: (1) $b = 2\text{mm}$ and $V = 3\text{mm}$ and (2) $b = 2\text{mm}$ and $V = 1\text{mm}$. These combinations are chosen because they represent extreme cases; similar results can be observed if a negative bias is used. It can be observed that the parameters from the least square fit converge to their true values. Unlike Bayesian inference, the effect of bias and noise is insignificant because as can be seen in Figure 4, the standard deviation is about the same for small and large noise after 1,500 cycles. However, the dark shades in Figure 4 show that there is a non negligible effect of noise when the maximum amplitude of the noise is larger than the bias. The convergence is slow when the crack size is small, and it is fast when the crack size is large. This happens because a larger crack has faster crack growth, which can also be observed in Bayesian inference.



(a) Distribution of identified a_i



(b) Distribution of identified m



(c) Distribution of identified $b/2$

Figure 4. . Distribution (mean \pm one standard deviation obtained using 1,000 sets of measurements) of fitted results of (a) a_0 , (b) m and (c) $b/2$

The main interest of prognosis is to predict the remaining useful life at inspection. In order to show the value of our method we compare RUL calculated using the actual value of m , m_{true} , and the critical value for both the initial and the updated distributions. Figure 5 shows the mean \pm one standard deviation of the 95% confidence of the distribution of remaining useful life for a bias of -2mm and a noise of maximum amplitude 1mm . The distribution took into account only uncertainty in measurements, and not the uncertainty in the identified parameters, thus leading to a very narrow distribution. It can be observed that least square fit leads to a very good identification of deterministic parameters and extrapolation of RUL but it does not give a very good estimation of the distribution of RUL and this leads to slightly unconservative results even for the 5th percentile. The estimated distribution of RUL

is narrow that if the mean is overestimated the 5th percentile might be as well. We have to note that the uncertainty in RUL results in this case only from the uncertainty in damage size estimation, it might be larger if the uncertainty in the estimated variables was included.

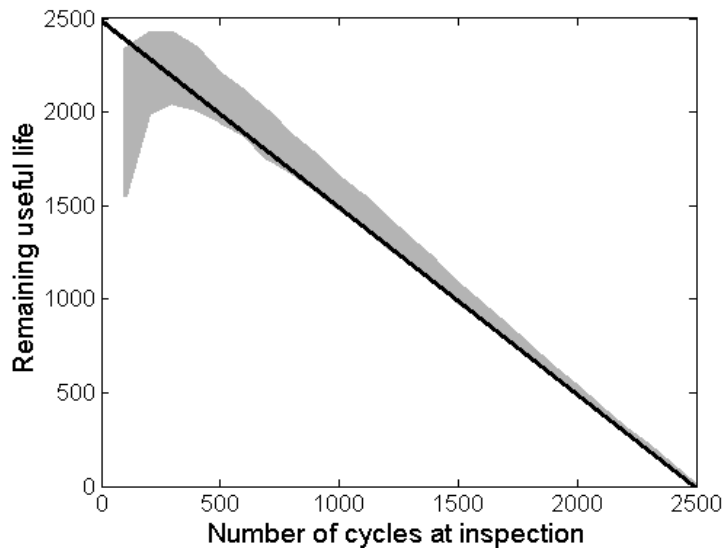


Figure 5. Distribution (mean \pm one standard deviation) 5th percentile of RUL for $b = -2\text{mm}$ and $V = 1\text{mm}$, using least square fit

Least-square-filtered Bayesian (LSFB) method for Characterizing Damage Growth Parameters

As described in the previous section, both Bayesian updating and least square fit present advantages and limitations, but they appear to be complementary. Least square fit ability to identify the bias and reduce the noise makes it a useful tool to process the data in order to identify the distribution of RUL using Bayesian updating.

In order to combine the advantages of the two methods, we propose to process information collected at every cycle by least square fit in order to reduce the noise, and identify the bias. The filtered data is then used in Bayesian updating in order to narrow down the distribution of m and obtain a more accurate prognosis.

Figure 6 illustrate one case showing the true crack size as the dashed line compared to the measurements at every inspection (stars) and the damage sizes obtained using least square fit (dots). The dots represent the data that in this method are used with Bayesian updating to update the distribution of m and estimate the distribution of RUL. Note that least square fit uses more data than the one illustrated in that figure, it uses data from every cycle.

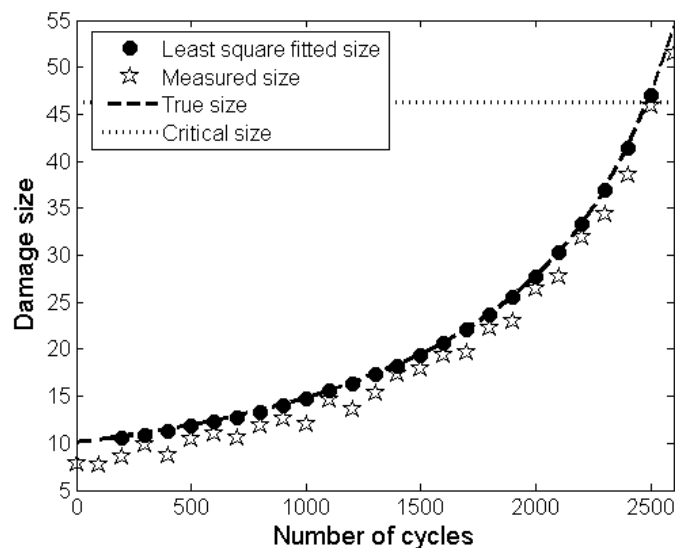


Figure 6. Comparison of the true, measured and fitted damage sizes for $b = -2\text{mm}$ and $V = 1\text{mm}$ Illustration with one simulated set of measurements.

Figure 6 illustrates the behavior of the crack over the entire life of the panel. Due to bias the general trend of the crack size is shifted down from the true crack size, and due to noise the crack growth is not consistent; in some cases, the measured crack size is reduced from the previous measurement. On the other hand, the estimated crack sizes using parameters from the least-square fit are close to the true crack sizes and show much more consistent behavior. Although SHM measurements are performed every cycle, data are shown at every 100th cycle in order to make consistent comparison with that of Bayesian inference. (b) on the other hand shows the behavior over two inspection intervals at the beginning and toward the end of life. It shows how the least square fit improves as the crack grows, as we have more information. But in both cases it can be observed that the fitted data are closer to the true values than the measured ones. This confirms the fact that least square fit reduces the effect of bias and noise.

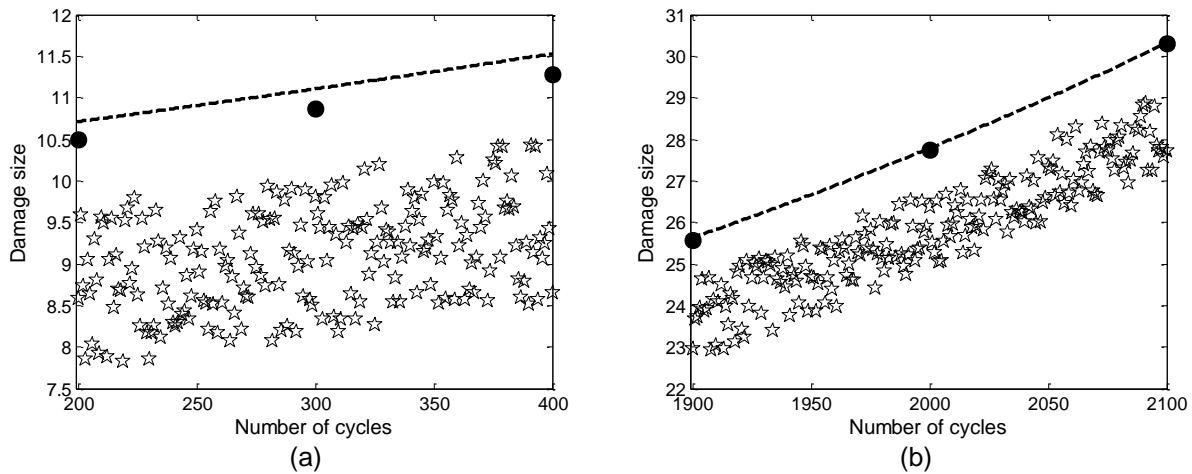


Figure 7. Fitted (dots) and measured (stars) damage at early and late stage in damage growth compared to the actual damage size (dotted line)

Figure 8 shows the results for the LSF method, the 5th percentile of remaining useful life obtained for data with a bias of -2 mm and a noise amplitude of 1 mm. It actually shows the mean of the percentile \pm one standard deviation obtained as for the previous methods using 100 sets of measurements. It can be observed that combining both methods gives better results than either of them separately. The estimation converges faster than with Bayesian updating but remains on the conservative side end is less sensitive to the errors in measurements.

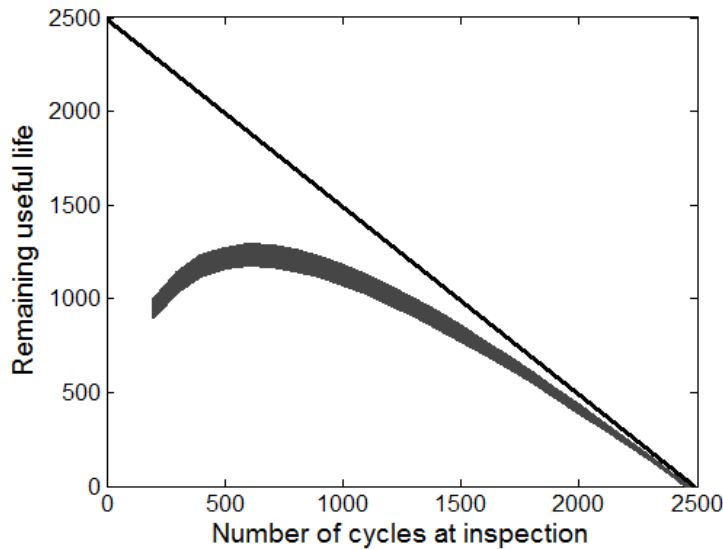


Figure 8. Distribution (mean \pm one standard deviation) 5th percentile of RUL for $b = -2\text{mm}$ and $V = 1\text{mm}$, using the combined method

Figure 9 compares the three methods presented in this paper. It can be observed that the LSF method is a good compromise between least square fit and Bayesian inference and it is much less sensitive to the noise in the data, the

variability in the distribution is much smaller. The conservative estimate of the RUL converges faster to the actual RUL than with Bayesian updating, but it remains always on the conservative side unlike with least square fit.

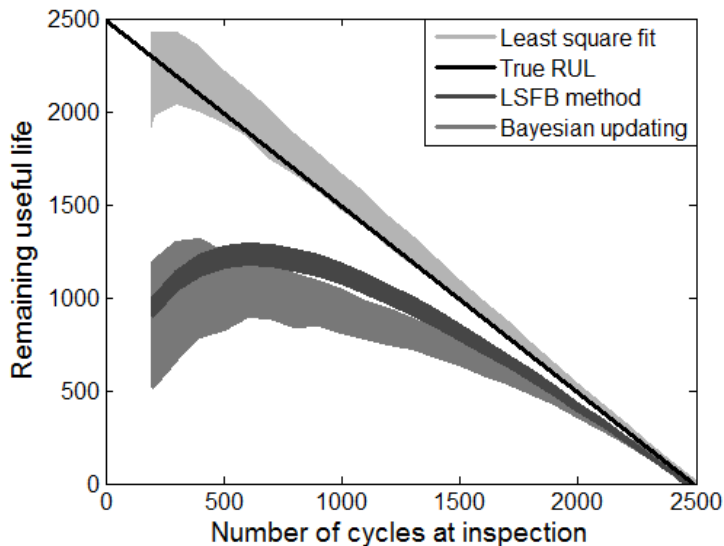


Figure 9. Comparison of the Distribution (mean \pm one standard deviation) 5th percentile of RUL using the three methods

V. Conclusions

We presented here prognosis results for three methods: Bayesian updating, least square fit, and a combination of both. Those results show that even though the first two methods are very good at identifying the damage growth parameters or estimating the remaining useful life, they both have limitations, they cannot do both. But they are complementary, such that they can be combined and by using the advantages of both methods we come up to a third one giving and estimation of RUL that converges to the actual RUL faster than Bayesian updating while remaining on the conservative side, unlike with least square fit. Another advantage of the combined method is that it is less sensitive to the errors in measurements. These conclusions can be best observed in Figure 9, it shows also that the combined method is much less sensitive to the error in the data.

Note that even though the results and conclusions presented in this paper are for a specific case of bias/noise combination similar results and conclusions can be obtained for other cases.

Appendix A – Derivation of the likelihood for Bayesian inference

The idea is to identify the damage parameters m or C from the measured half crack size that is contaminated by measurement errors. In order to do that, we compare the measurements to the simulated crack size defined above. In order to use the information in Bayes law, we need to estimate the likelihood $l(\Delta a|m)$ that for a given set of material properties m or C , $\Delta a_N^{meas} = \Delta a_N^{sim}$ or in other words:

$$d = \Delta a_N^{sim} - \Delta a_N^{meas} = 0 \quad (14)$$

If we have analytical expressions for the PDFs of a_N^{meas} and a_N^{sim} , and we use them to obtain the PDF of d , then the value of this PDF at $d = 0$ is the likelihood function. Since this rarely happens, we will use MCS, and we will use as likelihood function

$$l(\Delta a | m) = P \left[|d| \leq \epsilon \right] \quad (15)$$

Note that the integration over ϵ is just a normalizing constant that is taken care of by the normalization in the Bayesian formulation.

If we calculate $l(\Delta a|m)$ purely by sampling a_N^{meas} and a_N^{sim} , then the tolerance ϵ needs to be large enough to include enough sample points to reduce the sampling error to acceptable levels. On the other hand if ϵ is large, we will incur errors due to nonlinearity in the likelihood function.

We will assume now that the measurement error that controls a_N^{meas} is independent of the modeling errors that control a_N^{sim} . In that case, separable sampling can be performed by comparing all possible combinations of two individual samples.

The PDF of a_N^{sim} is not available analytically, because it is obtained from propagation of uncertainties through an analysis code. On the other hand, the measurement errors are assumed rather than propagated, and they are here assumed to be uniform in a bounded region. We will now investigate how we can take advantage of the given distribution of a_N^{meas} in order to improve the efficiency or accuracy of the sampling. In this case a_N^{meas} and a_N^{sim} are scalar, such that

$$l(\Delta a | m) = P \left| d \right| \leq \epsilon = 1 - P \quad d + \epsilon \leq 0 \quad -P \quad P - \epsilon \geq 0 \quad (16)$$

Using conditional expectation on the second term on the right-hand side we obtain

$$\begin{aligned} P \quad d - \epsilon \geq 0 &= P \quad \Delta a_N^{sim} - \Delta a_N^{meas} - \epsilon \geq 0 \\ &= \int_{\Delta a_N^{sim}} P \quad \Delta a_N^{sim} - \Delta a_N^{meas} - \epsilon \geq 0 \quad f_{sim} \quad \Delta a_N^{sim} \quad d\Delta a_N^{sim} \\ &= \int_{\Delta a_N^{sim}} F_{meas} \quad \Delta a_N^{sim} - \epsilon \quad f_{sim} \quad \Delta a_N^{sim} \quad d\Delta a_N^{sim} \end{aligned} \quad (17)$$

where $f_{sim}(x)$ is the PDF of Δa_N^{sim} and $F_{sim}(x)$ is the CDF of Δa_N^{sim} . The last relation is obtained from the definition of CDF; i.e., by considering Δa_N^{meas} as the only random variable, $P(\Delta a_N^{meas} \leq \Delta a_N^{sim} - \epsilon) = F_{meas}(\Delta a_N^{sim} - \epsilon)$. Similarly, the first term can be written as

$$\begin{aligned} P \quad d + \epsilon \geq 0 &= \int_{\Delta a_N^{sim}} P \quad \Delta a_N^{sim} - \Delta a_N^{meas} + \epsilon \geq 0 \quad f_{sim} \quad \Delta a_N^{sim} \quad d\Delta a_N^{sim} \\ &= \int_{\Delta a_N^{sim}} F_{meas} \quad \Delta a_N^{sim} + \epsilon \quad f_{sim} \quad \Delta a_N^{sim} \quad d\Delta a_N^{sim} \end{aligned} \quad (18)$$

Thus, by combining Eqs. (17) and (18), the likelihood can be written as

$$\begin{aligned} l(\Delta a | m) &= \int_{\Delta a_N^{sim}} \left[F_{meas} \quad \Delta a_N^{sim} + \epsilon - F_{meas} \quad \Delta a_N^{sim} - \epsilon \right] f_{sim} \quad \Delta a_N^{sim} \quad d\Delta a_N^{sim} \\ &\approx 2\epsilon \int_{\Delta a_N^{sim}} f_{meas} \quad \Delta a_N^{sim} \quad f_{sim} \quad \Delta a_N^{sim} \quad d\Delta a_N^{sim} \end{aligned} \quad (19)$$

where the central finite difference approximation is used in the second relation, which becomes exact when $\epsilon \rightarrow 0$. As explained before, since the posterior PDF will be normalized, the coefficient 2ϵ can be ignored. The above expression is in particular convenient for separable MCS because the analytical expression of $f_{meas}(x)$ is known, and $f_{sim}(x)$ can be evaluated by propagating uncertainty through numerical simulation. Let M be the number of samples in MCS, the likelihood can then be calculated by

$$\begin{aligned} l(\Delta a | m) &= \int_{\Delta a_N^{sim}} f_{meas}(\Delta a_N^{sim}) f_{sim}(\Delta a_N^{sim}) d\Delta a_N^{sim} \\ &\approx \frac{1}{M} \sum_{i=1}^M f_{meas}(\Delta a_{N,i}^{sim}) \end{aligned} \quad (20)$$

In the literature²⁹, Gaussian function is often assumed for the likelihood function. In addition, the expression of this function remains unchanged throughout the entire process. However, Figure 10 shows that the likelihood function is quite different from the Gaussian function and it varies at different crack sizes. Since the uncertainty structure of the posterior distribution strongly depends on the likelihood function in Bayesian inference, the error in the likelihood calculation directly affects the accuracy of the posterior distribution.

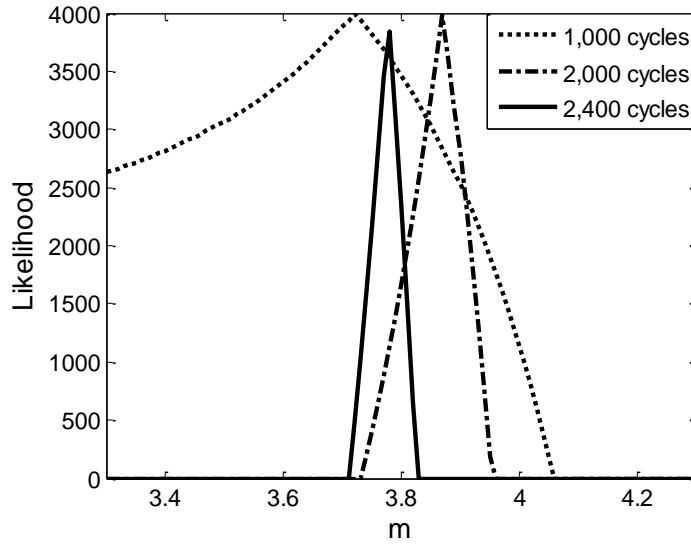


Figure 10. Likelihood function for one set of measurements at various number of cycles

In the case presented here $f_{meas}(a_{N-\Delta N,i}^{sim})$ is the PDF corresponding to the triangular distribution defined in Eq. (9). We give below the detailed algorithm of the Bayesian procedure at the N^{th} inspection

$$\begin{aligned}
 &\text{Input data: } a_{N-2\Delta N}^{meas}, \Delta a_N^{meas} \\
 &\quad \downarrow \text{Discretize } m \\
 &\quad \text{For every } m_i: \\
 &\quad \text{M samples of: } a_{N-2\Delta N}^{sim} = a_{N-2\Delta N}^{meas} + v_i \\
 &\quad \quad \text{With } v_i \sim U(-V, V) \\
 &a_N^{sim} = \left[\Delta NC \left(1 - \frac{m_i}{2}\right) (\sigma\sqrt{\pi})^{m_i} + (a_{N-\Delta N}^{sim})^{1-\frac{m_i}{2}} \right]^{\frac{2}{2-m_i}} \\
 &l(\Delta a | m_i) = \frac{1}{M} \sum_{i=1}^M f_{meas}(\Delta a_{N,i}^{sim})
 \end{aligned}$$

Acknowledgment

This work was supported by the Air Force Office of Scientific Research under Grant FA9550-07-1-0018 and by the NASA under Grant NNX08AC334.

References

- ¹Wang, L. and Yuan, F. G., "Damage identification in a composite plate using prestack reverse-time migration technique", *Structural Health Monitoring*, vol. 4, pp. 195-211, 2005.
- ²Luo, J., Namburu, M., Pattipati, K., Qiao, L., Kawamoto, M. and Chigusa S., "Model-based prognostic techniques [maintenance applications]", in *IEEE Systems Readiness Technology Conference*, 2003.
- ³Li, C. J. and Lee, H., "Gear fatigue crack prognosis using embedded model, gear dynamic model and fracture mechanics", *Mechanical systems and signal processing*, vol. 19, pp. 836-846, 2005.
- ⁴Berruet, P., Toguyeni, A. K. A. and Craye, E., "Structural and functional approach for dependability in FMS", in *IEEE International Conference on Systems, Man, and Cybernetics*, 1999.
- ⁵Ray, A. and Patankar, R., "A stochastic model of fatigue crack propagation under variable-amplitude loading", *Engineering Fracture Mechanics*, vol. 62, pp. 477-493, 1999.

- ⁶Ray, A. and Tangirala, S., “Stochastic modeling of fatigue crack dynamics for on-line failure prognostics”, *IEEE Transactions on Control Systems Technology*, vol. 4, pp. 443-451, 1996.
- ⁷Jaw, L. C., Inc, S. M. and Tempe, A. Z., “Neural networks for model-based prognostics”, in *IEEE Aerospace Conference*, 1999
- ⁸Schwabacher, M. A., “A survey of data-driven prognostics”, in *AIAA Infotech@Aerospace Conference*, Reston, VA, 2005.
- ⁹Montanari, G. C., “Aging and life models for insulation systems based on PD detection”, *IEEE Transactions on Dielectrics and Electrical Insulation*, vol. 2, pp. 667-675, 1995.
- ¹⁰Xue, Y., McDowell, D. L., Horstemeyer, M. F., Dale, M. H. and Jordon, J. B., “Microstructure-based multistage fatigue modeling of aluminum alloy 7075-T651”, *Engineering Fracture Mechanics*, vol. 74, pp. 2810-2823, 2007.
- ¹¹Goebel, K., Saha, B. and Saxena, A., “A comparison of three data-driven techniques for prognostics”, 2008.
- ¹²Srivastava, A. N. and Das, S., “Detection and Prognostics on Low Dimensional Systems”, *IEEE Transactions on Systems, Man, and Cybernetics, Part C: Applications and Reviews*, vol. 39, pp. 44-54, 2009.
- ¹³Tipping, M., *The Relevance Vector Machine. in Advances in Neural Information Processing Systems*, MIT Press, Cambridge, 2000.
- ¹⁴Yan, J. and Lee, J., “A Hybrid Method for On-line Performance Assessment and Life Prediction in Drilling Operations”, in *IEEE International Conference on Automation and Logistics*, 2007.
- ¹⁵Orchard, M., Kacprzyński, G., Goebel, K., Saha, B. and Vachtsevanos, G., “Advances in Uncertainty Representation and Management for Particle Filtering Applied to Prognostics”, in *International Conference on Prognostics and Health Management*, Denver, CO, 2008.
- ¹⁶Sheppard, J. W., Kaufman, M. A., Inc, A. and Annapolis, M. D., “Bayesian diagnosis and prognosis using instrument uncertainty”, *IEEE Autotestcon*, 2005, pp. 417-423.
- ¹⁷Saha, B. and Goebel, K., “Uncertainty Management for Diagnostics and Prognostics of Batteries using Bayesian Techniques”, in *IEEE Aerospace Conference*, 2008.
- ¹⁸Engel, S. J., Gilmartin, B. J., Bongort, K. and Hess, A., “Prognostics, the real issues involved with predicting liferemaining”, in *IEEE Aerospace Conference*, Big Sky, MT., March 18-25, 2000.
- ¹⁹Gu, J., Barker, D., and Pecht, M., “Uncertainty Assessment of Prognostics of Electronics Subject to Random Vibration”, in *AAAI Fall Symposium on Artificial Intelligence for Prognostics*, pp. 50-57, 2007.
- ²⁰Orchard, M., Wu, B. and Vachtsevanos, G., “A Particle Filter Framework for Failure Prognosis”, in *World Tribology Congress III*, Washington, D.C., 2005.
- ²¹DuQuesnay, D.L. and Underhill, P.R., “Fatigue life scatter in 7xxx series aluminum alloys”, *International Journal of Fatigue*, Elsevier, 2009.
- ²²Harkness, H. H., “Computational methods for fracture mechanics and probabilistic fatigue”. Ph.D. thesis, the Northwestern University, Evanston, IL, 199
- ²³Lin, K. Y., Rusk, D. T. and Du, J. J., “Equivalent level of safety approach to damage-tolerant aircraft structural design”, *Journal of Aircraft*, vol. 39, pp. 167-174, 2002.
- ²⁴Paris, P. C., Tada, H. and Donald, J. K., “Service load fatigue damage—a historical perspective”, *International Journal of fatigue*, vol. 21, pp. 35-46, 1999.
- ²⁵Niu, M., "Airframe Structural Design," in *Fatigue, Damage Tolerance and Fail-Safe Design*, Conmilit Press LTD., Ed. Hong Kong, pp. 538-570, 1990.
- ²⁶Newman, J. C., Phillips, E. P. and Swain, M. H., “Fatigue-life prediction methodology using small-crack theory”, *International Journal of fatigue*, vol. 21, pp. 109-119, 1999.
- ²⁷Carpinteri, A., Paggi, M., “Are the Paris' law parameters dependent on each other?” - *Frattura ed Integrità Strutturale*, 2008
- ²⁸An, J., Acar, E., Haftka, R. T., Kim, N. H., Ifju, P. G. and Johnson, T.F., “Being Conservative with a Limited Number of Test Results”, *Journal of Aircraft*, vol. 45, pp. 1969-1975, 2008.
- ²⁹Li, G., Yuan, F. G., Haftka, R. T. and Kim, N. H., “Bayesian segmentation for damage image using MRF prior”, *Sensors and Smart Structures Technologies for Civil, Mechanical, and Aerospace Systems, SPIE Conference*, San Diego, CA, USA vol. 7292 pp. 72920J-12, 2009